

Quantum asymptotic amplitude for quantum oscillatory systems from the Koopman operator viewpoint

Yuzuru Kato^{1, a)}

*Department of Complex and Intelligent Systems, Future University Hakodate,
Hokkaido 041-8655, Japan*

(Dated: 12 August 2025)

We have recently proposed a fully quantum-mechanical definition of the asymptotic phase for quantum nonlinear oscillators, which is also applicable in the strong quantum regime [Kato and Nakao 2022 Chaos 32 063133]. In this study, we propose a definition of the quantum asymptotic amplitude for quantum oscillatory systems, which naturally extends the asymptotic amplitude for classical nonlinear oscillators on the basis of the Koopman operator theory. We introduce the asymptotic amplitude for quantum oscillatory systems by using the eigenoperator of the backward Liouville operator associated with the largest non-zero real eigenvalue. Using examples of the quantum van der Pol oscillator with the quantum Kerr effect, which exhibits quantum limit-cycle oscillations, and the quantum van der Pol model with the quantum squeezing and degenerate parametric oscillator with nonlinear damping, which exhibit quantum noise-induced oscillations, we demonstrate that the proposed quantum asymptotic amplitude yields isostable amplitude values that decay exponentially with a constant rate. Furthermore, using the quantum asymptotic amplitude, we introduce effective quantum periodic orbits for quantum limit-cycle oscillations and quantum noise-induced oscillations.

^{a)}Electronic mail: Corresponding author: katoyuzu@fun.ac.jp

I. INTRODUCTION

Rhythmic oscillations are ubiquitous in nature and have been extensively studied in a wide range of classical systems, including heartbeats, circadian rhythms, chemical oscillations, and electrical oscillators¹⁻⁶. With recent advances in quantum technology, a theoretical model of quantum rhythmic oscillations^{7,8} has been proposed and their novel features have been extensively studied⁷⁻³⁵. In addition, experimental observations of phase synchronization between quantum rhythmic oscillations have also been reported³⁶⁻³⁸.

Rhythmic oscillations in classical deterministic systems can be modeled as nonlinear dynamical systems with stable limit-cycle solutions. The concepts of *asymptotic phase* and *isochron*¹⁻⁵, which exhibits a linear increase with a constant frequency within the basin of attraction of the limit cycle, are commonly used for analyzing synchronization phenomena. The asymptotic phase, originally introduced by Winfree³⁹ and Guckenheimer⁴⁰ from a geometrical perspective^{39,40}, has been shown to be closely related to the Koopman eigenfunction associated with the fundamental oscillation frequency⁴¹⁻⁴⁶.

From the Koopman perspective, the concepts of *asymptotic amplitudes* and *isostables*, which characterize deviation from the limit cycle and exhibit exponential decay with constant rates toward the limit cycle, have been naturally introduced in terms of the Koopman eigenfunction associated with the Floquet exponents having non-zero real parts⁴¹⁻⁴⁷. These phase and amplitude functions are fundamental quantities for characterizing limit-cycle oscillations. Moreover, when the system dynamics are dominated by slow modes⁴², a common feature in realistic oscillator models⁴⁸, a phase-amplitude reduction can be applied^{41-46,48,49}. This reduction technique provides a useful framework for analyzing and controlling synchronization dynamics.

The phase and amplitude description can also be extended to classical stochastic oscillatory systems. The stochastic asymptotic phase⁵⁰, which exhibits a linear increase with a constant frequency on average under the system's stochastic dynamics, has been introduced using the slowest-decaying eigenfunction of the backward Fokker-Planck (Kolmogorov) operator. Similarly, the stochastic asymptotic amplitude⁵¹, which decays exponentially with a constant rate on average under the system's stochastic dynamics, has been introduced based on the eigenfunction associated with the largest non-zero real eigenvalue. These definitions of stochastic asymptotic phase and amplitude are closely related to stochastic Koopman

operator theory⁵²⁻⁵⁴ and can be viewed as natural extensions of their deterministic counterparts defined based on Koopman eigenfunctions⁵⁵. Moreover, the zero-level set of the stochastic asymptotic amplitude defines a periodic orbit associated with the stochastic oscillatory dynamics⁵¹. When the deterministic part of the system possesses a stable limit cycle, this zero-level set coincides with the limit-cycle attractor in the noiseless limit.

By extending the definition of the stochastic asymptotic phase from the Koopman operator viewpoint, we recently introduced a definition of *the quantum asymptotic phase* for quantum oscillatory systems. This quantum asymptotic phase exhibits linear increase under the system's quantum dynamics and provides isochronous phase values for analyzing quantum synchronization even in the strong quantum regime^{32,33}. However, the concept of *quantum asymptotic amplitude* for quantum oscillatory systems remains unexplored, and quantum periodic orbits associated with quantum oscillatory dynamics are not yet well characterized.

In this study, we introduce a definition of the quantum asymptotic amplitude for quantum oscillatory systems by extending the concept of the stochastic asymptotic amplitude from the Koopman operator viewpoint. Specifically, the quantum asymptotic amplitude is defined in terms of the eigenoperator of the backward Liouville operator associated with the largest non-zero real eigenvalue. Using examples such as the quantum van der Pol oscillator with the quantum Kerr effect, which exhibits quantum limit-cycle oscillations, and the quantum van der Pol model with quantum squeezing, as well as the degenerate parametric oscillator with nonlinear damping, which exhibit quantum noise-induced oscillations, we numerically demonstrate that the proposed quantum asymptotic amplitude yields appropriate amplitude values that decay exponentially at a constant rate under quantum system dynamics. Furthermore, based on the quantum asymptotic amplitude, we introduce effective quantum periodic orbits for both quantum limit-cycle oscillations and noise-induced oscillations, which characterize the quantum oscillatory behavior that inherently reflects quantum effects.

II. ASYMPTOTIC AMPLITUDE FOR QUANTUM OSCILLATORY SYSTEMS

In this section, we provide a brief overview of quantum oscillatory systems, review the quantum asymptotic phase introduced in Ref.³², and present a definition of the quantum asymptotic amplitude.

A. Quantum oscillatory systems

We consider an open quantum system that exhibits oscillatory behavior. Assuming that the interactions between the system and its reservoirs occur instantaneously, we adopt the Markovian approximation. Under this assumption, the time evolution of the system's density operator ρ is governed by the quantum master equation⁵⁶⁻⁵⁸

$$\dot{\rho} = \mathcal{L}\rho = -i[H, \rho] + \sum_{j=1}^n \mathcal{D}[C_j]\rho, \quad (1)$$

where $\dot{(\)}$ denotes the time derivative, \mathcal{L} denotes a Liouville superoperator governing the evolution of ρ , H denotes a system Hamiltonian, C_j denotes a coupling operator between the system and the j th reservoir ($j = 1, \dots, n$), $[A, B] = AB - BA$ denotes the commutator, $\mathcal{D}[C]\rho = C\rho C^\dagger - (\rho C^\dagger C + C^\dagger C\rho)/2$ denotes the Lindblad form where \dagger indicates the Hermitian conjugate, and we set the reduced Planck's constant as $\hbar = 1$.

We introduce an inner product $\langle X, Y \rangle_{tr} = \text{Tr}(X^\dagger Y)$ of linear operators X and Y and define the superoperator \mathcal{L}^* , the adjoint of \mathcal{L} , such that it satisfies $\langle \mathcal{L}^* X, Y \rangle_{tr} = \langle X, \mathcal{L} Y \rangle_{tr}$, which can be explicitly expressed as

$$\mathcal{L}^* X = i[H, X] + \sum_{j=1}^n \mathcal{D}^*[C_j]X, \quad (2)$$

where $\mathcal{D}^*[C]X = C^\dagger X C - (X C^\dagger C + C^\dagger C X)/2$ is the adjoint Lindblad form.

The superoperator \mathcal{L}^* governs the evolution of an observation operator F through the equation

$$\dot{F} = \mathcal{L}^* F. \quad (3)$$

In the Schrödinger picture, the density operator ρ evolves according to Eq. (1), whereas the observation operator F remains constant. Conversely, in the Heisenberg picture, F

evolves according to Eq. (3), whereas ρ remains constant. In both pictures, the expectation value of F with respect to ρ , namely,

$$\langle F \rangle_q = \text{Tr}(\rho F) = \langle \rho, F \rangle_{tr} \quad (4)$$

remains the same value (ρ is self-adjoint).

The Liouville superoperator \mathcal{L} possesses a biorthogonal eigensystem $\{\Lambda_k, U_k, V_k\}_{k=0,1,2,\dots}$, which consists of the eigenvalue Λ_k and eigenoperators U_k and V_k , satisfying

$$\mathcal{L}U_k = \Lambda_k U_k, \quad \mathcal{L}^*V_k = \overline{\Lambda_k} V_k, \quad \langle V_k, U_l \rangle_{tr} = \delta_{kl}, \quad (5)$$

for $k, l = 0, 1, 2, \dots$, where the overline denotes the complex conjugate.

We assume that one eigenvalue, denoted Λ_0 , equals zero, corresponding to the stationary state ρ_0 of the system, namely $\mathcal{L}\rho_0 = 0$, and that all other eigenvalues have negative real parts. This assumption also implies the absence of decoherence-free subspaces⁵⁹. Furthermore, we assume that the eigenvalues with the smallest absolute real part, that is, those associated with the slowest decay rate, form a complex-conjugate pair,

$$\Lambda_1 = \mu_q - i\Omega_q, \quad \overline{\Lambda_1} = \mu_q + i\Omega_q, \quad (6)$$

where $|\mu_q|$ ($\mu_q < 0$) represents the decay rate, and $\Omega_q = \text{Im } \overline{\Lambda_1}$ represents the frequency of the fundamental oscillation. With these assumptions, the system exhibits oscillatory behavior.

B. Phase-space representation

We can transform the density operator ρ into a quasiprobability distribution in the phase space^{56,57,60}. By employing the P -representation^{56,57,60}, the density operator ρ is expressed as

$$\rho = \int p(\boldsymbol{\alpha}) |\alpha\rangle \langle \alpha| d\boldsymbol{\alpha}, \quad (7)$$

where $|\alpha\rangle$ represents a coherent state characterized by a complex value α , or a complex vector $\boldsymbol{\alpha} = (\alpha, \bar{\alpha})^T$, the function $p(\boldsymbol{\alpha})$ represents a quasiprobability distribution of $\boldsymbol{\alpha}$, $d\boldsymbol{\alpha} = d\alpha d\bar{\alpha}$, and the integral is taken over the whole complex plane.

Similarly, we transform the observable F into a function in the phase space as

$$f(\boldsymbol{\alpha}) = \langle \alpha | F | \alpha \rangle, \quad (8)$$

where the operator F is arranged in the normal order^{56,57,60}. Introducing the L^2 inner product $\langle g(\boldsymbol{\alpha}), h(\boldsymbol{\alpha}) \rangle_{\alpha} = \int \overline{g(\boldsymbol{\alpha})} h(\boldsymbol{\alpha}) d\boldsymbol{\alpha}$ for two functions $g(\boldsymbol{\alpha})$ and $h(\boldsymbol{\alpha})$, we express the expectation value of F with respect to ρ as

$$\langle F \rangle_q = \text{Tr}(\rho F) = \int d\boldsymbol{\alpha} p(\boldsymbol{\alpha}) f(\boldsymbol{\alpha}) = \langle p(\boldsymbol{\alpha}), f(\boldsymbol{\alpha}) \rangle_{\alpha}. \quad (9)$$

We describe the time evolution of $p(\boldsymbol{\alpha})$, which corresponds to Eq. (1), by a partial differential equation

$$\partial_t p(\boldsymbol{\alpha}) = L_{\alpha} p(\boldsymbol{\alpha}), \quad (10)$$

where the differential operator L_{α} satisfies $\mathcal{L}\rho = \int L_{\alpha} p(\boldsymbol{\alpha}) |\alpha\rangle\langle\alpha| d\boldsymbol{\alpha}$. We can explicitly derive L_{α} from Eq. (1) using the correspondence of the quantum operator to the differential operator in the phase-space representation^{56,57}. In the Heisenberg picture, correspondingly, the evolution of $f(\boldsymbol{\alpha})$ is similarly described by

$$\partial_t f(\boldsymbol{\alpha}) = L_{\alpha}^+ f(\boldsymbol{\alpha}), \quad (11)$$

where the differential operator L_{α}^+ denotes the adjoint of L_{α} with respect to the L^2 inner product, namely, $\langle L_{\alpha}^+ g(\boldsymbol{\alpha}), h(\boldsymbol{\alpha}) \rangle_{\alpha} = \langle g(\boldsymbol{\alpha}), L_{\alpha} h(\boldsymbol{\alpha}) \rangle_{\alpha}$, which satisfies $L_{\alpha}^+ f(\boldsymbol{\alpha}) = \langle\alpha|\mathcal{L}^*F|\alpha\rangle$.

The differential operator L_{α} possesses a biorthogonal eigensystem $\{\Lambda_k, U_k, V_k\}_{k=0,1,2,\dots}$, which consists of the eigenvalue Λ_k and eigenfunctions $u_k(\boldsymbol{\alpha})$ and $v_k(\boldsymbol{\alpha})$, satisfying

$$L_{\alpha} u_k = \Lambda_k u_k, \quad L_{\alpha}^+ v_k = \overline{\Lambda_k} v_k, \quad \langle v_k, u_l \rangle_{\alpha} = \delta_{kl}. \quad (12)$$

This eigensystem corresponds one-to-one with Eq. (5). The eigenvalues $\{\Lambda_k\}_{k \geq 0}$ are identical to those of \mathcal{L} . The eigenfunctions u_k and v_k of L_{α} and L_{α}^+ are linked to the eigenoperators U_k and V_k of \mathcal{L} and \mathcal{L}^* , respectively, as

$$U_k = \int u_k(\boldsymbol{\alpha}) |\alpha\rangle\langle\alpha| d\boldsymbol{\alpha}, \quad v_k(\boldsymbol{\alpha}) = \langle\alpha|V_k|\alpha\rangle, \quad (13)$$

which are obtained from $\mathcal{L}U_k = \int u_k(\boldsymbol{\alpha}) \{\mathcal{L}|\alpha\rangle\langle\alpha|\} d\boldsymbol{\alpha} = \int \{L_{\alpha} u_k(\boldsymbol{\alpha})\} |\alpha\rangle\langle\alpha| d\boldsymbol{\alpha} = \int \Lambda_k u_k(\boldsymbol{\alpha}) |\alpha\rangle\langle\alpha| d\boldsymbol{\alpha} = \Lambda_k U_k$ and $L_{\alpha}^+ v_k = L_{\alpha}^+ \langle\alpha|V_k|\alpha\rangle = \langle\alpha|\mathcal{L}^*V_k|\alpha\rangle = \overline{\Lambda_k} \langle\alpha|V_k|\alpha\rangle = \overline{\Lambda_k} v_k$.

C. Quantum asymptotic phase

Before introducing the quantum asymptotic amplitude, we briefly review the quantum asymptotic phase as introduced in Ref.³².

In Ref.³², we introduced the quantum asymptotic phase $\Phi_q(\rho)$ of a quantum state ρ as the argument of the expectation value of the eigenoperator V_1 associated with the eigenvalue $\overline{\Lambda_1}$ as

$$\Phi_q(\rho) = \arg\langle V_1 \rangle_q = \arg\langle \rho, V_1 \rangle_{tr} = \arg\langle p(\boldsymbol{\alpha}), v_1(\boldsymbol{\alpha}) \rangle_{\boldsymbol{\alpha}}. \quad (14)$$

This quantum asymptotic phase increases with a constant frequency Ω_q when the quantum state evolves according to Eq.(1), namely,

$$\frac{d}{dt}\Phi_q(\rho) = \Omega_q. \quad (15)$$

In particular, the asymptotic phase of the coherent state $\rho^\alpha = |\alpha\rangle\langle\alpha|$ can be regarded as a quantum asymptotic phase $\Phi_q(\boldsymbol{\alpha})$ of the coherent state $\boldsymbol{\alpha}$ in the P representation, expressed as

$$\Phi_q(\boldsymbol{\alpha}) = \arg\langle \rho^\alpha, V_1 \rangle_{tr} = \arg v_1(\boldsymbol{\alpha}) = \arg\langle \alpha | V_1 | \alpha \rangle. \quad (16)$$

The quantum asymptotic phase naturally extends from the stochastic asymptotic phase, which is introduced in terms of the slowest decaying eigenfunction of the backward Kolmogorov (Fokker-Planck) operator⁵⁰ and coincides with the deterministic asymptotic phase in the noiseless limit from the Koopman operator viewpoint⁵⁵. Indeed, when the quantum system in the classical limit possesses a stable-limit cycle attractor, the quantum asymptotic phase coincides with the deterministic asymptotic phase in the classical limit³².

D. Quantum asymptotic amplitude

The aim of this study is to introduce a definition of the quantum asymptotic amplitude by extending the concept of the stochastic asymptotic amplitude⁵¹, in a manner analogous to the definition of the quantum asymptotic phase.

For the asymptotic amplitude, we select the largest non-zero real eigenvalue, denoted by $\kappa_q = \Lambda_2$, considering it characterizes the decay rate of the asymptotic amplitude of the system (see also Fig. 1(a) and Fig. 2).

We define the quantum asymptotic amplitude $R_q(\rho)$ of the quantum state ρ as the expectation value of the eigenoperator V_2 , which is associated with the eigenvalue $\kappa_q (= \Lambda_2)$, as

$$R_q(\rho) = \langle p(\boldsymbol{\alpha}), v_2(\boldsymbol{\alpha}) \rangle_{\boldsymbol{\alpha}} = \langle \rho, V_2 \rangle_{tr}. \quad (17)$$

We can confirm that the asymptotic amplitude $R_q(\rho)$ evolves with a constant rate κ_q under the time evolution of the quantum state ρ as governed by Eq.(1),

$$\begin{aligned} \frac{d}{dt}R_q(\rho) &= \left\langle \frac{\partial p(\boldsymbol{\alpha})}{\partial t}, v_2(\boldsymbol{\alpha}) \right\rangle_{\boldsymbol{\alpha}} = \langle L_{\alpha} p(\boldsymbol{\alpha}), v_2(\boldsymbol{\alpha}) \rangle_{\boldsymbol{\alpha}} = \langle p(\boldsymbol{\alpha}), L_{\alpha}^+ v_2(\boldsymbol{\alpha}) \rangle_{\boldsymbol{\alpha}} \\ &= \langle p(\boldsymbol{\alpha}), \kappa_q v_2(\boldsymbol{\alpha}) \rangle_{\boldsymbol{\alpha}} = \kappa_q \langle p(\boldsymbol{\alpha}), v_2(\boldsymbol{\alpha}) \rangle_{\boldsymbol{\alpha}} = \kappa_q R_q(\rho), \end{aligned} \quad (18)$$

or equivalently,

$$\begin{aligned} \frac{d}{dt}R_q(\rho) &= \langle \dot{\rho}, V_2 \rangle_{tr} = \langle \mathcal{L}\rho, V_2 \rangle_{tr} = \langle \rho, \mathcal{L}^* V_2 \rangle_{tr} \\ &= \langle \rho, \kappa_q V_2 \rangle_{tr} = \kappa_q \langle \rho, V_2 \rangle_{tr} = \kappa_q R_q(\rho). \end{aligned} \quad (19)$$

Integrating over time, we obtain

$$R_q(\rho) = \exp(\kappa_q t) R_q(\rho_0), \quad (20)$$

where ρ_0 is the initial state at $t = 0$. Thus, the asymptotic amplitude $R_q(\rho)$ decays exponentially with a constant rate κ_q when the quantum state ρ evolves according to Eq. (1).

Analogous to the quantum asymptotic phase, the asymptotic amplitude of the coherent state $\rho^{\alpha} = |\alpha\rangle\langle\alpha|$ can be interpreted as a quantum asymptotic amplitude $R_q(\boldsymbol{\alpha})$ of the coherent state $\boldsymbol{\alpha}$ in the P representation, expressed as

$$R_q(\boldsymbol{\alpha}) = \langle \rho^{\alpha}, V_2 \rangle_{tr} = v_2(\boldsymbol{\alpha}) = \langle \alpha | V_2 | \alpha \rangle. \quad (21)$$

The quantum asymptotic amplitude extends naturally from the asymptotic amplitude of the stochastic oscillators, which is introduced in terms of the eigenfunction of the backward Kolmogorov (Fokker-Planck) operator⁵¹ associated with the largest non-zero real eigenvalue, and coincides with the deterministic asymptotic amplitude in the noiseless limit from the Koopman operator viewpoint⁵⁵.

Moreover, we introduce the effective quantum periodic orbit χ_q as the zero-level set of the quantum asymptotic amplitude, namely,

$$\chi_q = \{\boldsymbol{\alpha} | R_q(\boldsymbol{\alpha}) = 0\}, \quad (22)$$

when this set forms a periodic orbit. When the quantum system in the classical limit possesses a stable-limit cycle attractor, this effective quantum periodic orbit coincides with the deterministic limit-cycle trajectory in the classical limit.

It is important to note that the quantum asymptotic phase $\Phi_q(\rho)$ and amplitude $R_q(\rho)$ of the quantum state ρ can be directly derived from the quantum master equation without resorting to the phase space representation. We employed the P function to introduce the quantum asymptotic phase $\Phi_q(\alpha)$ and amplitude $R_q(\alpha)$ of the coherent state α since these functions are easily derived from the eigenoperators in numerical calculations. Additionally, we note that typical observables in quantum optics are often expressed in normal order, and their expectation values can be conveniently evaluated using the P-function⁵⁶.

III. NUMERICAL RESULTS

To validate the proposed quantum asymptotic amplitude, we consider several representative quantum oscillatory systems that can introduce corresponding deterministic trajectories in the classical limit. First, we examine the quantum van der Pol oscillator with the quantum Kerr effect, which exhibits quantum limit-cycle oscillations in both the semiclassical and strong quantum regimes. Next, we investigate the quantum van der Pol model with quantum squeezing, which exhibits quantum noise-induced oscillations near the saddle-node on invariant circle (SNIC) bifurcation in the classical limit^{6,61}, and a degenerate parametric oscillator with nonlinear damping, which exhibits quantum noise-induced oscillations near a pitchfork bifurcation in the classical limit^{6,61}. We also analyze a harmonic oscillator with linear damping in Appendix B.

In our numerical calculations, we use the truncated matrix representation of the Liouville superoperator and compute the asymptotic phase and amplitude in Eqs. (16) and (21) from the eigensystem of this matrix³². When illustrating the quantum asymptotic phase, we select the sign of Ω_q such that the asymptotic phase exhibits a counterclockwise increase.

A. Quantum van der Pol model with the quantum Kerr effect

As a first example, we consider the quantum van der Pol oscillator with the quantum Kerr effect. The quantum master equation of the system is described by^{12,32}

$$\dot{\rho} = \mathcal{L}\rho = -i[H, \rho] + \gamma_1 \mathcal{D}[a^\dagger]\rho + \gamma_2 \mathcal{D}[a^2]\rho, \quad (23)$$

where a and a^\dagger denote the annihilation and creation operators, respectively. The Hamiltonian is defined as $H = \omega_0 a^\dagger a + K a^{\dagger 2} a^2$, where ω_0 represents the frequency of the oscillator,

K is the Kerr parameter, and γ_1 and γ_2 represent the decay rates for negative damping and nonlinear damping, respectively.

1. *Semiclassical regime*

First, we consider the system in the semiclassical regime where γ_2 and K are sufficiently smaller than γ_1 . In this regime, the quantum master equation in Eq. (23) is described by the quantum Fokker-Planck equation for $p(\boldsymbol{\alpha})$ in Eq. (10), and the system state is approximately described by a corresponding stochastic differential equation representing the deterministic trajectory subjected to the small quantum noise in the phase space^{11,32}.

Figure 1(a) shows the numerically obtained eigenvalues of \mathcal{L}^* in the vicinity of the imaginary axis, where the real eigenvalue with the largest real part κ_q is marked with a red dot ($\kappa_q < 0$) and the eigenvalue $\overline{\Lambda}_1$ with the smallest absolute real part is marked with a yellow dot. In this semiclassical regime, the eigenvalue $\overline{\Lambda}_1 = \mu_q + i\Omega_q$ ($\mu_q < 0$) lies on the rightmost light-blue branch of the eigenvalues, which is approximately characterized by a parabola $\hat{\lambda}_n = i\Omega_q n + \mu_q n^2$ ($n = 0, \pm 1, \pm 2, \dots$) passing through $\overline{\Lambda}_1$. Therefore, we focus on the slowest-decaying mode with the eigenvalue $\overline{\Lambda}_1$ because their imaginary parts are essentially integer multiples of Ω_q .

In the classical limit, where quantum noise vanishes, the system is characterized by a complex variable $\alpha \in \mathbb{C}$, which evolves according to a deterministic system derived from the drift term of the approximate quantum Fokker-Planck equation for $p(\boldsymbol{\alpha})$ (see the details in Appendix B in Ref.³²),

$$\dot{\alpha} = \left(\frac{\gamma_1}{2} - i\omega_0 \right) \alpha - (\gamma_2 + 2Ki)\bar{\alpha}\alpha^2. \quad (24)$$

This model is known as the Stuart-Landau oscillator, the normal form of the supercritical Hopf bifurcation², and has a stable limit-cycle χ_c . This limit-cycle attractor is explicitly calculated as $\alpha_c(\phi) = r_c e^{i\phi}$, where $\phi = \Omega_c t + \text{const.}$ with a natural frequency $\Omega_c = -\omega_0 - K\gamma_1/\gamma_2$ and $r_c = \sqrt{\gamma_1/2\gamma_2}$ (accordingly, the quantum van der Pol model is also referred to as the quantum Stuart-Landau model in recent literature^{13,27}). The basin of attraction of this limit cycle is the entire complex plane, excluding the origin.

Figure 2 presents a schematic diagram illustrating the eigenvalues of L_α^+ , or \mathcal{L}^* , when the system approaches the deterministic system in the classical limit with a stable limit-cycle

solution. In the classical limit, the eigenvalues take the form $\lambda_c = m\kappa_c + in\Omega_c$ ($m = 0, 1, 2, \dots$ and $n = 0, \pm 1, \pm 2$), with $\kappa_c = -\gamma_1$ representing the largest non-zero real eigenvalue and $i\Omega_c$ representing the pure-imaginary eigenvalue with the smallest absolute imaginary part. When the system approaches the deterministic system in the classical limit, the eigenvalues related to the asymptotic phase and amplitude, which appear in curved branches in the semiclassical regime in Fig. 2(a), converge to those in the corresponding straight branches of eigenvalues in the classical limit in Fig. 2(b).

The classical asymptotic amplitude R_c of the system, associated with the eigenvalue κ_c in the classical limit, is calculated as⁵⁵

$$R_c(\boldsymbol{\alpha}) = c_0 \left(\gamma_2 - \frac{\gamma_1}{2(x^2 + p^2)} \right), \quad (25)$$

where $(x, p) = (\text{Re } \alpha, \text{Im } \alpha)$ and c_0 is an arbitrary real constant because the scale of the asymptotic amplitude can be freely chosen. The amplitude satisfies $\dot{R}_c(\boldsymbol{\alpha}) = \kappa_c R_c(\boldsymbol{\alpha})$ when α evolves within the basin of attraction of the limit cycle under Eq. (24).

Figures 1(b) and 1(c) illustrate the quantum asymptotic amplitude $|R_q(\boldsymbol{\alpha})|$ and the corresponding asymptotic amplitude $|R_c(\boldsymbol{\alpha})|$, respectively. Both amplitude functions are scaled by a constant factor such that the maximum value of $|R_q|$ becomes 1, and the same color map is used in both figures. In Fig. 1(c), values of $|R_c|$ greater than 1 near the origin are illustrated in the same color. In Fig. 1(b), the red-thin line illustrates the effective quantum periodic orbit χ_q , and in Fig. 1(c), the orange-thin line illustrates the deterministic limit cycle $\chi_c (= \{\boldsymbol{\alpha} | R_c(\boldsymbol{\alpha}) = 0\})$ in the classical limit. The quantum asymptotic amplitude $R_q(\rho) (= \langle p(\boldsymbol{\alpha}), R_q(\boldsymbol{\alpha}) \rangle_{\boldsymbol{\alpha}})$ of the quantum state ρ decays exponentially to zero, indicating that the system evolves toward the vicinity of the effective quantum periodic orbit χ_q . In the classical limit, the quantum periodic orbit χ_q coincides with the classical limit cycle χ_c . Therefore, in this regime with sufficiently small quantum noise, the quantum periodic orbit χ_q closely matches the classical limit-cycle χ_c .

In Fig. 1(d), we also plot the quantum asymptotic phase $\Phi_q(\boldsymbol{\alpha})$ together with the effective quantum periodic orbit χ_q . The phase increases in the counterclockwise direction along the quantum periodic orbit.

To confirm that the quantum asymptotic amplitude produces appropriate amplitude values, we numerically evaluate the free relaxation of ρ starting from an initial coherent state $\rho_0 = |\alpha_0\rangle\langle\alpha_0|$ with $\alpha_0 = 1$ at $t = 0$. We evaluate $r_q = |R_q(\rho)| = |\langle \rho, V_2 \rangle_{tr}|$ of the eigenop-

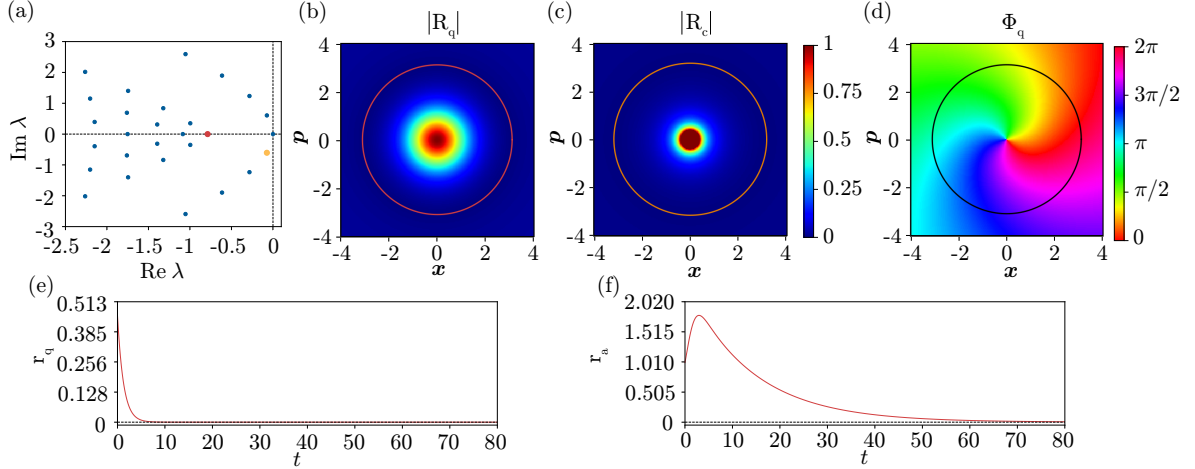


FIG. 1. Quantum asymptotic amplitude of a quantum van der Pol oscillator with the quantum Kerr effect in the semiclassical quantum regime, for $\gamma_1 = 1$ and $(\omega_0, \gamma_2, K)/\gamma_1 = (0.1, 0.05, 0.025)$. (a) Eigenvalues of \mathcal{L}^* in the vicinity of the imaginary axis. The red dot represents the largest non-zero real eigenvalue κ_q , and the yellow dot represents the principal eigenvalue $\overline{\Lambda}_1$. (b) Quantum asymptotic amplitude $|R_q|$ with $\kappa_q = -0.787$. (c) Classical asymptotic amplitude $|R_c|$ with $\kappa_c = -1$. (d) Quantum asymptotic phase Φ_q with $\Omega_q = -0.605$. (e-f) Evolution of r_q and r_a : (e) r_q , (f) r_a . The red-thin line in (b) and the black-thin line in (d) represent the effective quantum periodic orbit χ_q . The orange-thin line in (c) represents the deterministic limit cycle χ_c in the classical limit. In (d), the phase origin is set at $(x, p) = (2.5, 0)$.

erator V_2 and compare it with $r_a = |\langle a \rangle_q| = |\langle \rho, a \rangle_{tr}|$ of the annihilation operator a , which represents the polar radius of $\langle a \rangle$ on the complex plane. Due to dissipation, the system evolves from the initial pure coherent state into a mixed state and eventually reaches a stationary mixed state. Figures 1(e) and 1(f) depict the time evolution of r_q and r_a , respectively. The asymptotic amplitude r_q decays exponentially with a constant rate κ_q in Fig. 1(e). In contrast, the radius r_a does not exhibit an exponential decay over time; particularly, it increases during the transient evolution before $t = 5$ in Fig. 1(f). These results confirm that, in the semiclassical regime, the quantum asymptotic amplitude provides an appropriate and consistent amplitude values.

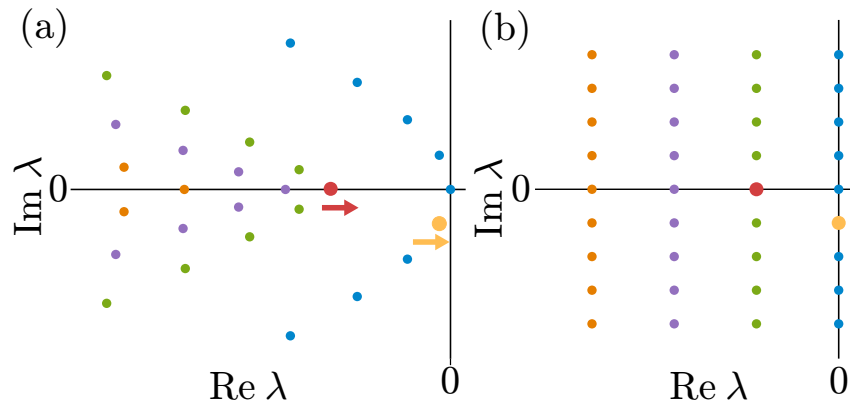


FIG. 2. A schematic diagram illustrating eigenvalues of L_{α}^+ when approaching to the classical limit. (a) Semiclassical regime. (b) Classical limit. The red and yellow dots represent the eigenvalues related to the asymptotic amplitude and phase, respectively.

2. Strong quantum regime

Next, we consider the strong quantum regime, where γ_2 and K are relatively large compared to γ_1 . In this regime, the system dynamics is dominated by a small number of energy states and the semiclassical approximation becomes inapplicable.

Figure 3(a) shows the numerically obtained eigenvalues of \mathcal{L}^* in the vicinity of the imaginary axis, with κ_q marked with a red dot and $\overline{\Lambda}_1$ marked with a yellow dot.

Figures 3(b) and 3(c) depict the quantum asymptotic amplitude $|R_q(\alpha)|$ and the corresponding asymptotic amplitude $|R_c(\alpha)|$, respectively, where both amplitude functions are scaled by a constant factor such that the maximum value of $|R_q|$ becomes 1, the same color map is applied to both figures, and values of $|R_c|$ exceeding 1 near the origin in Fig. 3(c) are illustrated in the same color. The effective quantum periodic orbit χ_q and the deterministic limit cycle χ_c in the classical limit are plotted by the red-thin line in Fig. 3(b) and the orange-thin line in Fig. 3(c), respectively. In the strong quantum regime, the quantum periodic orbit χ_q clearly deviates from the classical limit cycle χ_c .

In Fig. 3(d), we also plot the quantum asymptotic phase $\Phi_q(\alpha)$ together with the effective quantum periodic orbit χ_q , where the phase increases in the counterclockwise direction along the quantum periodic orbit.

We numerically evaluate the free relaxation of ρ , starting from an initial coherent state $\rho_0 = |\alpha_0\rangle\langle\alpha_0|$ with $\alpha_0 = 1$ at $t = 0$, and plot the time evolution of the asymptotic amplitude

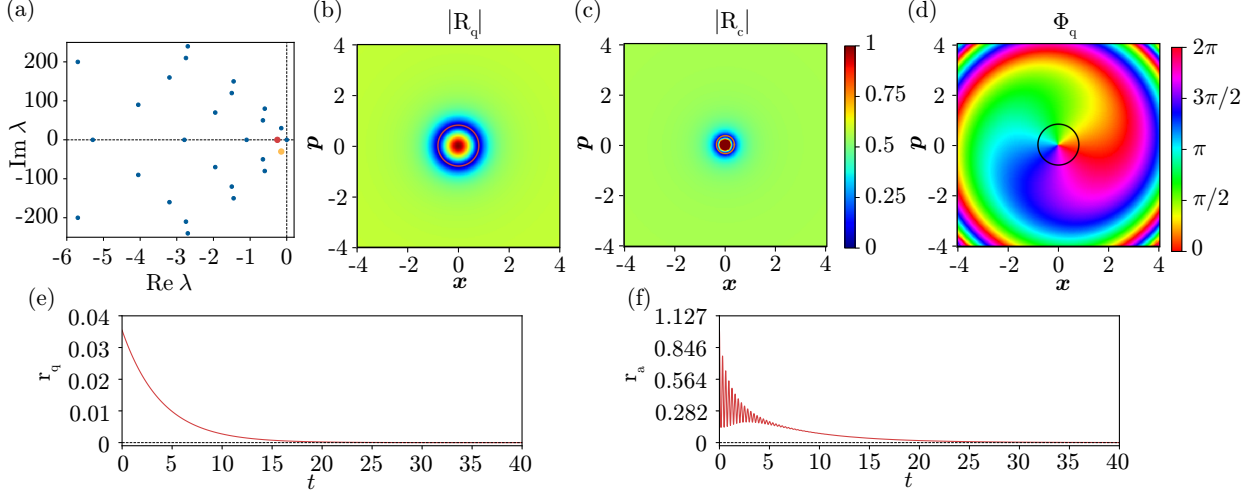


FIG. 3. Quantum asymptotic amplitude of a quantum van der Pol oscillator with the quantum Kerr effect in the strong quantum regime, for $\gamma_1 = 0.1$ and $(\omega_0, \gamma_2, K)/\gamma_1 = (300, 4, 100)$. (a) Eigenvalues of \mathcal{L}^* in the vicinity of the imaginary axis. The red dot represents the largest non-zero real eigenvalue κ_q , and the yellow dot represents the principal eigenvalue $\overline{\Lambda}_1$. (b) Quantum asymptotic amplitude $|R_q|$ with $\kappa_q = -0.256$. (c) Classical asymptotic amplitude $|R_c|$ with $\kappa_c = -0.1$. (d) Quantum asymptotic phase Φ_q with $\Omega_q = -30$. (e-f) Evolution of r_q and r_a : (e) r_q , (f) r_a . The red-thin line in (b) and the black-thin line in (d) represent the effective quantum periodic orbit χ_q . The orange-thin line in (c) represents the deterministic limit cycle χ_c in the classical limit. In (d), the phase origin is set at $(x, p) = (2.5, 0)$.

r_q and radius r_a . Figures 3(e) and (f) depict the time evolution of r_q and r_a , respectively. As expected, the asymptotic amplitude r_q exhibits an exponential decay with a constant rate κ_q . In contrast, the radius r_a does not decay exponentially but instead oscillates rapidly over time. These results indicate that, despite strong quantum effects significantly altering the system dynamics from the classical limit, the quantum asymptotic amplitude R_q reliably produces isostable amplitude values even in the strong quantum regime.

B. Quantum van der Pol model with the quantum squeezing

Next, we consider a system exhibiting quantum noise-induced oscillations, i.e., oscillatory responses excited by quantum noise⁶². Specifically, we consider a system in the classical limit

lies near an SNIC bifurcation^{6,61}. As a minimum model exhibiting such quantum noise-induced oscillations, we consider a quantum van der Pol model subjected to the quantum squeezing⁹. In the classical limit, the corresponding deterministic system behaves as an excitable bistable system slightly below the bifurcation point of spontaneous limit-cycle oscillations⁶².

Let ω_{sq} denote the frequency of the pump beam of the quantum squeezing. In the rotating coordinate frame with frequency $\omega_{sq}/2$, the system evolves according to the following quantum master equation^{9,11,62}

$$\dot{\rho} = -i [-\Delta a^\dagger a + i\eta(a^2 e^{-i\theta} - a^{\dagger 2} e^{i\theta}), \rho] + \gamma_1 \mathcal{D}[a^\dagger]\rho + \gamma_2 \mathcal{D}[a^2]\rho, \quad (26)$$

where, $\Delta = \omega_{sq}/2 - \omega_0$ denotes the detuning of the half frequency of the pump beam of squeezing from the system's oscillatory frequency, and $\eta e^{i\theta}$ ($\eta \geq 0$, $0 \leq \theta < 2\pi$) denotes the squeezing parameter.

In the classical limit, where the quantum noise vanishes, the system is described by a complex variable $\alpha \in \mathbb{C}$, which evolves according to the deterministic system (see the derivation in Appendix A)

$$\dot{\alpha} = \left(\frac{\gamma_1}{2} + i\Delta\right) \alpha - \gamma_2 \bar{\alpha} \alpha^2 - 2\eta e^{i\theta} \bar{\alpha}. \quad (27)$$

By using the modulus R and argument ϕ of the complex variable $\alpha = R e^{i\phi}$, the differential equations for these variables are obtained by

$$\dot{R} = \frac{\gamma_1}{2} R - \gamma_2 R^3 - 2\eta R \cos(2\phi - \theta), \quad (28)$$

$$\dot{\phi} = \Delta + 2\eta \sin(2\phi - \theta). \quad (29)$$

When the squeezing effect is present, i.e., $\eta \neq 0$, the system has two stable fixed points for $\Delta \leq 2\eta$, as seen in the equation for the argument ϕ in Eq. (29). These fixed points annihilate with their corresponding unstable fixed points via an SNIC bifurcation at $\Delta = 2\eta$; a stable limit-cycle emerges and the argument ϕ continuously increases over time when $\Delta > 2\eta$, whereas ϕ has two stable fixed points and converges to one of them depending on the initial state when $\Delta < 2\eta$. When the system in the classical limit is slightly below the onset of the SNIC bifurcation, namely, when Δ is slightly less than 2η , oscillatory response can be induced by the quantum noise. In what follows, we consider such a parameter configuration (see Appendix A for details).

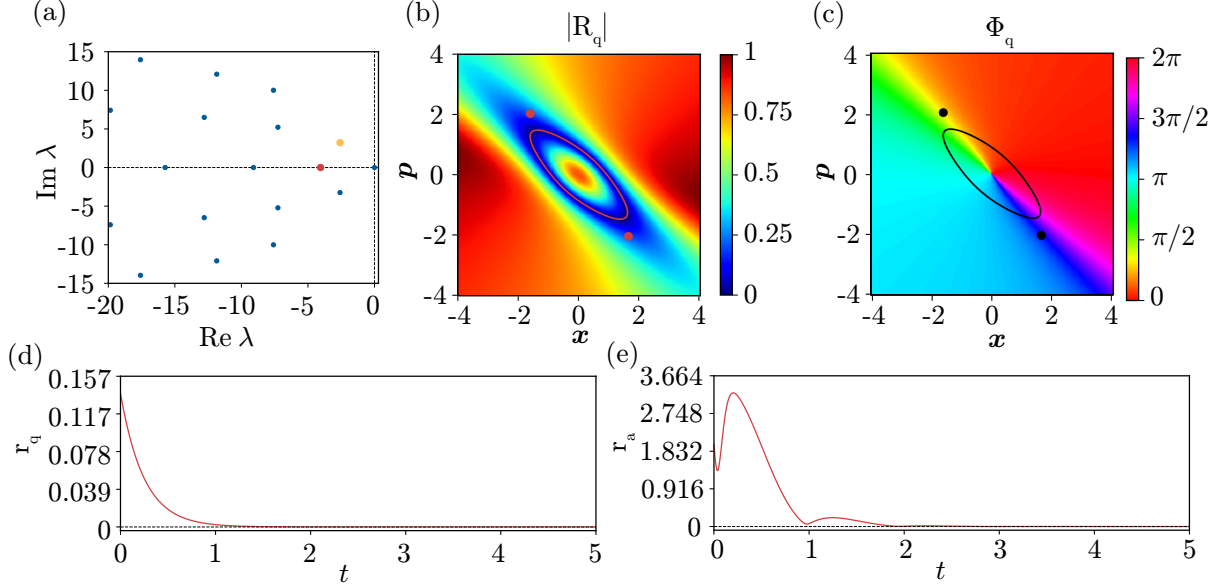


FIG. 4. Quantum asymptotic amplitude of a quantum van der Pol model with the quantum squeezing effect, for $\gamma_1 = 1$ and $(\Delta, \gamma_2, \eta)/\gamma_1 = (13.65, 0.53, 7)$. (a) Eigenvalues of \mathcal{L}^* in the vicinity of the imaginary axis. The red dot represents the largest non-zero real eigenvalue κ_q , and the yellow dot represents the principal eigenvalue $\overline{\Lambda}_1$. (b) Quantum asymptotic amplitude $|R_q|$ with $\kappa_q = -4.052$. (c) Quantum asymptotic phase Φ_q with $\Omega_q = 3.248$. (d,e) Evolution of r_q and r_a : (d) r_q , (e) r_a . The red-thin line in (b) and the black-thin line in (c) represent the effective quantum periodic orbit χ_q , and the two red dots in (b) and the two black dots in (c) represent the two stable fixed points in the classical limit. In (c), the phase origin is set at $(x, p) = (2.5, 0)$.

Figure 4(a) shows the numerically obtained eigenvalues of \mathcal{L}^* in the vicinity of the imaginary axis, with κ_q marked with a red dot and $\overline{\Lambda}_1$ marked with a yellow dot.

Figures 4(b) and 4(c) depict the quantum asymptotic amplitude $|R_q(\boldsymbol{\alpha})|$ and phase $\Phi_q(\boldsymbol{\alpha})$, respectively, where the amplitude function is scaled by a constant factor such that the maximum value of $|R_q|$ becomes 1. Although the system in the classical limit is set below the SNIC bifurcation and only possesses two stable fixed points, which are shown by the two red dots in Fig. 4(b) and two black dots in Fig. 4(c), the oscillatory response excited by the quantum noise gives rise to an effective quantum periodic orbit χ_q , which is illustrated by the red-thin line in Fig. 4(b) and black-thin line in Fig. 4(c). This effective quantum periodic orbit is illustrated using the quantum asymptotic amplitude and cannot be introduced from the deterministic dynamics of the system in the classical limit.

The quantum asymptotic phase $\Phi_q(\boldsymbol{\alpha})$ can also be introduced using Eq. (16), which increases in the counterclockwise direction along the effective quantum periodic orbit χ_q , as depicted in Fig. 4(c). The quantum asymptotic phase captures the underlying fast-slow dynamics corresponding to the round trip between two stable fixed points, with slow dynamics (rapid phase change) near the two stable fixed points and fast dynamics (moderate phase change) between them, as depicted in Fig. 4(c). It should be noted that this is the first illustration of an asymptotic phase for a quantum noise-induced oscillation.

We consider the free relaxation of ρ from an initial coherent state $\rho_0 = |\alpha_0\rangle\langle\alpha_0|$ with $\alpha_0 = 2$ at $t = 0$ and plot the time evolution of the asymptotic amplitude r_q and the radius r_a . Figures 4(d) and (e) depict the time evolution of r_q and r_a , respectively. As expected, the asymptotic amplitude r_q decays exponentially with a constant rate κ_q . In contrast, the radius r_a does not exhibit an exponential decay over time; instead, it increases during the transient evolution before $t = 2$.

C. A degenerate parametric oscillator with nonlinear damping

Next, we consider another system exhibiting quantum noise-induced oscillations; particularly, we consider a system in the classical limit to be near a pitchfork bifurcation^{6,61}. As a minimum model exhibiting such quantum noise-induced oscillations, we consider a degenerate parametric oscillator with nonlinear damping^{63,64}, whose deterministic system in the classical limit can exhibit a pitchfork bifurcation.

The pump beam for the squeezing is also added in this model. In the rotating coordinate frame with a frequency of $\omega_{sq}/2$, the system dynamics are governed by the following quantum master equation^{63,64}

$$\dot{\rho} = -i [-\Delta a^\dagger a + i\eta(a^2 e^{-i\theta} - a^{\dagger 2} e^{i\theta}), \rho] + \gamma_2 \mathcal{D}[a^2]\rho + \gamma_3 \mathcal{D}[a]\rho, \quad (30)$$

where γ_3 represents the decay rate for linear damping.

In the classical limit, where the quantum noise vanishes, the system is characterized by a single complex variable $\alpha \in \mathbb{C}$, which evolves according to a deterministic system (see the derivation in Appendix A)

$$\dot{\alpha} = \left(\frac{-\gamma_3}{2} + i\Delta \right) \alpha - \gamma_2 \bar{\alpha} \alpha^2 - 2\eta e^{i\theta} \bar{\alpha}. \quad (31)$$

Using the modulus R and argument ϕ of the complex variable $\alpha = Re^{i\phi}$, the differential equations for these variables are given by

$$\dot{R} = \frac{-\gamma_3}{2}R - \gamma_2 R^3 - 2\eta R \cos(2\phi - \theta), \quad (32)$$

$$\dot{\phi} = \Delta + 2\eta \sin(2\phi - \theta). \quad (33)$$

When the squeezing effect is present, i.e., $\eta \neq 0$, the equation for the argument in Eq. (33), possesses two stable fixed points for $\Delta \leq 2\eta$. In this case, a non-zero positive solution of the equation for the modulus in Eq. (32) arises via a pitchfork bifurcation at $\eta = \frac{1}{2}\sqrt{\frac{\gamma_3^2}{4} + \Delta^2}$; the system possesses two stable fixed points with a common modulus when $\eta > \frac{1}{2}\sqrt{\frac{\gamma_3^2}{4} + \Delta^2}$, while it possesses a single stable fixed point at the origin when $\eta \leq \frac{1}{2}\sqrt{\frac{\gamma_3^2}{4} + \Delta^2}$.

We assume that the equation for the modulus in Eq. (32) is slightly below the bifurcation, namely $\eta < \frac{1}{2}\sqrt{\frac{\gamma_3^2}{4} + \Delta^2}$, and the equation for the argument in Eq. (33) is slightly below the bifurcation, namely $\Delta < 2\eta$. In this case, due to the effect of quantum noise, the system can exceed the pitchfork bifurcation point, leading to the emergence of two stable fixed points. Simultaneously, it exceeds the bifurcation point $\Delta = 2\eta$ of the argument and exhibits an oscillatory response characterized by the round trip around two emerging stable fixed points, resulting in a quantum noise-induced oscillation starting from the origin. In what follows, we consider such a parameter configuration (see the details in Appendix A).

Figure 5(a) shows the numerically obtained eigenvalues of \mathcal{L}^* in the vicinity of the imaginary axis, with κ_q marked with a red dot and $\overline{\Lambda}_1$ marked with a yellow dot.

Figures 5(b) and 5(c) depict the quantum asymptotic amplitude $|R_q(\boldsymbol{\alpha})|$ and phase $\Phi_q(\boldsymbol{\alpha})$, respectively, where the amplitude function is scaled by a constant factor such that the maximum value of $|R_q|$ becomes 1. Although the system in the classical limit is set below a pitchfork bifurcation and has only a stable fixed point at the origin, which is shown by the red dot in Fig. 5(b) and black dot in Fig. 5(c), the oscillatory response excited by the quantum noise leads to the emergence of an effective quantum periodic orbit χ_q , which is illustrated by the red-thin line in Fig. 5(b) and black-thin line in Fig. 5(c). This effective quantum periodic orbit is illustrated using the proposed quantum asymptotic amplitude and cannot be introduced from the deterministic dynamics of the system in the classical limit.

The quantum asymptotic phase $\Phi_q(\boldsymbol{\alpha})$ can also be introduced using Eq. (16), which increases in the counterclockwise direction along the effective quantum periodic orbit χ_q , as depicted in Fig. 5(c). The quantum asymptotic phase reflects fast-slow dynamics, similar

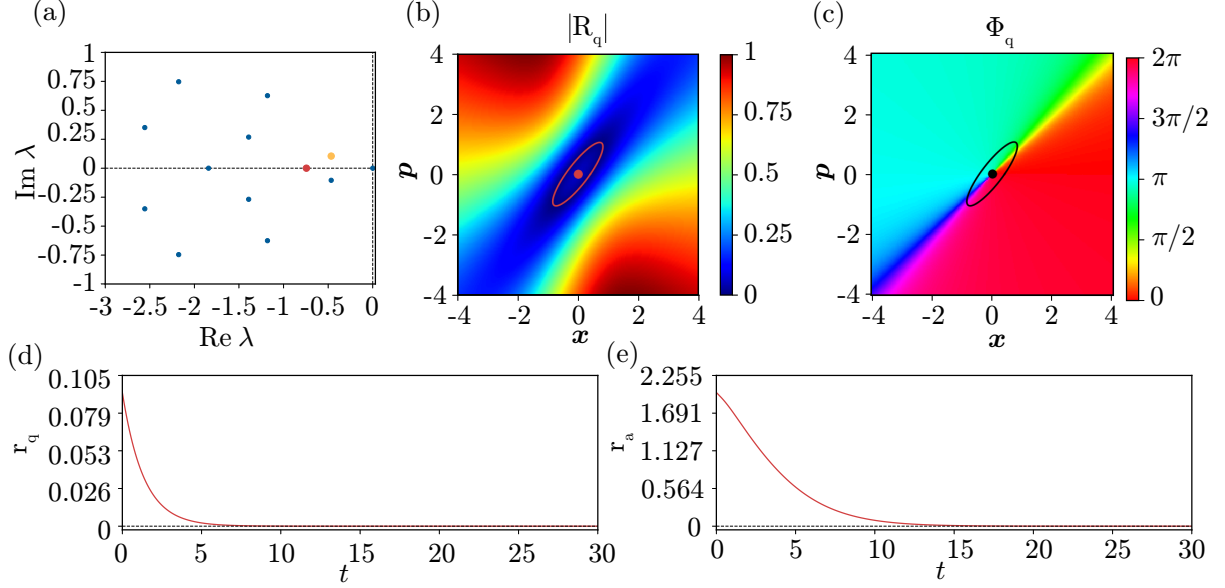


FIG. 5. Quantum asymptotic amplitude of a degenerate parametric oscillator with nonlinear damping, for $\gamma_2 = 0.1$ and $(\Delta, \gamma_3, \eta e^{-i\theta})/\gamma_2 = (6, 7.5, -3.25)$. (a) Eigenvalues of \mathcal{L}^* in the vicinity of the imaginary axis. The red dot represents the largest non-zero real eigenvalue κ_q , and the yellow dot represents the principal eigenvalue $\bar{\Lambda}_1$. (b) Quantum asymptotic amplitude $|R_q|$ with $\kappa_q = -0.744$. (c) Quantum asymptotic phase Φ_q with $\Omega_q = 0.105$. (d,e) Evolution of r_q and r_a : (d) r_q , (e) r_a . The red-thin line in (b) and the black-thin line in (c) represent the effective quantum periodic orbit χ_q , and the red dot in (b) and the black dot in (c) represent the stable fixed point at the origin in the classical limit. In (c), the phase origin is set at $(x, p) = (2.5, 0)$.

to the behavior observed in Fig. 4(c), which corresponds to the noise-induced oscillations starting from the origin.

We consider the free relaxation of ρ from an initial coherent state $\rho_0 = |\alpha_0\rangle\langle\alpha_0|$ with $\alpha_0 = 2$ at $t = 0$ and plot the time evolution of the asymptotic amplitude r_q and the radius r_a . Figures 5(d) and (e) illustrate the time evolution of r_q and r_a , respectively. As expected, the asymptotic amplitude r_q decays exponentially with a constant rate κ_q . In contrast, the radius r_a does not exhibit an exponential decay over time.

Note that similar noise-induced oscillations can also arise in classical stochastic systems when its noiseless deterministic dynamics lies slightly below a pitchfork bifurcation. In analogy with previous studies on quasicycles occurring below a supercritical Hopf bifurcation in the corresponding deterministic systems⁶⁵, these oscillations can be interpreted as

quasicycles emerging below a pitchfork bifurcation.

D. Discussion

In this study, we focused on asymptotic amplitude functions for quantum oscillatory systems exhibiting quantum limit-cycle oscillations and quantum noise-induced oscillations. In classical deterministic systems, asymptotic amplitudes, also referred to as isostables, can be defined even for linear systems with stable fixed points^{41,43}. Similarly, the quantum asymptotic amplitude can be introduced for quantum oscillatory systems, even when their classical counterparts do not exhibit, or are not near, bifurcations associated with nonlinear oscillations. As demonstrated in Appendix B, we explicitly compute the asymptotic amplitude function for a quantum harmonic oscillator with linear damping, a linear system that does not exhibit nonlinear oscillatory behavior.

For deterministic classical nonlinear systems possessing a stable limit-cycle solution, the zero-level set of the asymptotic amplitude function coincides with the stable limit cycle χ_c . Hence, the effective quantum periodic orbit χ_q , which is defined as the zero-level set of the quantum asymptotic amplitude, can be regarded as a natural generalization of the limit-cycle attractor for quantum nonlinear oscillatory systems. As shown in the examples in Sec. III A 2, this effective quantum periodic orbit can also be introduced even in the strong quantum regime and may be used for formulating a phase reduction theory for quantum synchronization beyond the semiclassical regime. Moreover, we can also introduce the effective quantum periodic orbit in examples of quantum noise-induced oscillations in Sec. III B and III C. This effective quantum periodic orbit cannot be derived without introducing the quantum asymptotic amplitude and offers intuitive insights into the dynamics of quantum oscillatory systems in the phase space of quasiprobability distribution.

The asymptotic amplitude characterizes the magnitude of the slowest decaying mode and captures the slowest asymptotic approach of the system to its steady state. Accordingly, it differs from the conventional notion of amplitude, i.e., the radius, associated with oscillators. Moreover, the asymptotic amplitude is conceptually distinct from the amplitude equations used in pattern formation theory⁶⁶, which describe the dynamics of unstable modes near bifurcation points through differential equations for complex variables.

In this study, our focus is solely on the eigenfunction associated with the largest non-zero

real eigenvalue to introduce the quantum asymptotic amplitude. Recently, regarding the slowest-decaying eigenfunction of the backward Fokker-Planck (Kolmogorov) operator, not only the argument used for defining the stochastic asymptotic phase, but also the modulus of the eigenfunction is used for formulating a universal description of stochastic oscillators⁶⁷. Moreover, eigenfunctions associated with dominant eigenvalues from different eigenvalue branches can be used to introduce multiple quantum asymptotic phases for analyzing quantum synchronization in the strong quantum regimes³³. Thus, besides the eigenfunctions associated with the largest non-zero real eigenvalue, the modulus of the other dominant eigenfunctions, which also exhibit exponential decay, may also provide valuable information for analyzing quantum oscillatory systems in the strong quantum regime.

IV. CONCLUSIONS

We introduced a definition of the asymptotic amplitude for quantum oscillatory systems by extending the asymptotic amplitude for classical stochastic oscillatory systems from the Koopman operator viewpoint⁵⁵. The quantum asymptotic amplitude produces appropriate isostable amplitude values and introduces effective quantum periodic orbits for quantum limit-cycle oscillations and quantum noise-induced oscillations. Despite increasing interest in quantum synchronization, the theoretical tools for analyzing quantum rhythmic oscillations and synchronization remain less developed than those for classical systems. When combined with the quantum asymptotic phase introduced in our previous work³², the proposed quantum asymptotic amplitude, applicable even in strong quantum regime, may offer novel tools for qualitatively analyzing quantum synchronization.

In this study, we focused on quantum nonlinear oscillators in quantum optical systems due to their clear correspondence with classical nonlinear oscillatory systems. Recently, quantum limit-cycle oscillations in quantum spin systems have been investigated through their corresponding deterministic dynamics in the classical limit⁶⁸. In particular, we have recently proposed the quantum spin van der Pol oscillator, which exhibits a classical limit-cycle trajectory corresponding to the normal form of a supercritical Hopf bifurcation⁶⁹. Therefore, as a future study, our definitions of quantum asymptotic phase and amplitude functions also need to be investigated for quantum oscillatory systems in the quantum spin systems and may be used for analyzing quantum spin synchronization^{15,26}.

Recently, a phase reduction theory for quantum nonlinear oscillators, applicable even in the strong quantum regime, has been developed based on the stochastic Schrödinger equation. This formulation relies on the limit-cycle trajectory reconstructed via quantum continuous measurement³⁴. By utilizing the proposed quantum asymptotic phase, amplitude, and effective quantum periodic orbit, it may be possible to formulate a phase-amplitude reduction theory for quantum nonlinear oscillators directly from the quantum master equation. Such a framework would reduce the full quantum dynamics into phase and amplitude equations, thereby simplifying the analysis of quantum oscillatory behavior and enabling a systematic analysis of quantum synchronization in the strong quantum regime.

Beyond the analysis of quantum nonlinear oscillatory systems, the Koopman operator perspective may open a new avenue for studying open quantum systems. Notably, Koopman operator theory for classical Hamiltonian systems was originally inspired by the operator formalism of quantum Hamiltonian systems⁷⁰. With recent progress in applying Koopman operator theory to classical dissipative systems⁴³, extending this framework to quantum dissipative, or open quantum, systems presents a promising direction for the detailed analysis, control, and optimization of complex quantum nonlinear dynamics.

ACKNOWLEDGMENTS

The authors gratefully acknowledge stimulating discussions with Hiroya Nakao. Numerical simulations have been performed by using QuTiP numerical toolbox^{71,72}. We acknowledge JSPS KAKENHI JP22K14274, JST PRESTO JP-MJPR24K3 and JST CREST JP-MJCR1913 for financial support.

Conflict of Interest

The authors have no conflicts to disclose.

Data availability

The data that supports the findings of this study are available within the article.

Appendix A: Models exhibiting noise-induced oscillations in the semiclassical regime

In this section, we briefly explain the classical limit of the models exhibiting quantum noise-induced oscillations discussed in Sec. III B, and III C. To present these models in a unified manner, we consider the following quantum master equation,

$$\dot{\rho} = -i [-\Delta a^\dagger a + i\eta(a^2 e^{-i\theta} - a^{\dagger 2} e^{i\theta}), \rho] + \gamma_1 \mathcal{D}[a^\dagger]\rho + \gamma_2 \mathcal{D}[a^2]\rho + \gamma_3 \mathcal{D}[a]\rho, \quad (\text{A1})$$

In the semiclassical regime, the linear operator L_α in Eq. (10) can be described by a Fokker-Planck operator,

$$L_\alpha = \left[-\sum_{j=1}^2 \partial_j \{A_j(\alpha)\} + \frac{1}{2} \sum_{j=1}^2 \sum_{k=1}^2 \partial_j \partial_k \{D_{jk}(\alpha)\} \right] \quad (\text{A2})$$

where $\partial_1 = \partial/\partial\alpha$ and $\partial_2 = \partial/\partial\bar{\alpha}$.

The drift vector $\mathbf{A}(\alpha) = (A_1(\alpha), A_2(\alpha))^\top \in \mathbb{C}^2$ and the matrix $\mathbf{D}(\alpha) = (D_{jk}(\alpha)) \in \mathbb{C}^{2 \times 2}$ are given by

$$\mathbf{A}(\alpha) = \begin{pmatrix} \left(\frac{\gamma_1 - \gamma_3}{2} + i\Delta\right) \alpha - \gamma_2 \bar{\alpha} \alpha^2 - 2\eta e^{i\theta} \bar{\alpha} \\ \left(\frac{\gamma_1 - \gamma_3}{2} - i\Delta\right) \bar{\alpha} - \gamma_2 \alpha \bar{\alpha}^2 - 2\eta e^{-i\theta} \alpha \end{pmatrix}, \quad (\text{A3})$$

$$\mathbf{D}(\alpha) = \begin{pmatrix} -(\gamma_2 \alpha^2 + 2\eta e^{i\theta}) & \gamma_1 \\ \gamma_1 & -(\gamma_2 \bar{\alpha}^2 + 2\eta e^{-i\theta}) \end{pmatrix}. \quad (\text{A4})$$

The corresponding SDE of the system, representing the deterministic trajectory subjected to the small quantum noise in the phase space, is given by

$$d \begin{pmatrix} \alpha \\ \bar{\alpha} \end{pmatrix} = \begin{pmatrix} \left(\frac{\gamma_1 - \gamma_3}{2} + i\Delta\right) \alpha - \gamma_2 \bar{\alpha} \alpha^2 - 2\eta e^{i\theta} \bar{\alpha} \\ \left(\frac{\gamma_1 - \gamma_3}{2} - i\Delta\right) \bar{\alpha} - \gamma_2 \alpha \bar{\alpha}^2 - 2\eta e^{-i\theta} \alpha \end{pmatrix} dt + \boldsymbol{\beta}(\alpha) \begin{pmatrix} dW_1 \\ dW_2 \end{pmatrix}, \quad (\text{A5})$$

where W_1 and W_2 are independent Wiener processes, and the matrix $\boldsymbol{\beta}(\alpha)$ is written as

$$\boldsymbol{\beta}(\alpha) = \begin{pmatrix} \sqrt{\frac{(\gamma_1 + R_{11}(\alpha))}{2}} e^{i\chi_{11}(\alpha)/2} & -i\sqrt{\frac{(\gamma_1 - R_{11}(\alpha))}{2}} e^{i\chi_{11}(\alpha)/2} \\ \sqrt{\frac{(\gamma_1 + R_{11}(\alpha))}{2}} e^{-i\chi_{11}(\alpha)/2} & i\sqrt{\frac{(\gamma_1 - R_{11}(\alpha))}{2}} e^{-i\chi_{11}(\alpha)/2} \end{pmatrix}, \quad (\text{A6})$$

where $R_{11}(\alpha) e^{i\chi_{11}(\alpha)} = -(\gamma_2 \alpha^2 + 2\eta e^{i\theta})$. The two equations for α and $\bar{\alpha}$ in Eq. (A5) are complex conjugate and describe the same dynamics.

In the classical limit, where the quantum noise vanishes, the system is characterized by a single complex variable $\alpha \in \mathbb{C}$, which obeys the deterministic part of Eq. (A5), given by

$$\dot{\alpha} = \left(\frac{\gamma_1 - \gamma_3}{2} + i\Delta \right) \alpha - \gamma_2 \bar{\alpha} \alpha^2 - 2\eta e^{i\theta} \bar{\alpha}. \quad (\text{A7})$$

Using the modulus R and argument ϕ of the complex variable $\alpha = Re^{i\phi}$, the differential equations for these variables are given by

$$\dot{R} = \frac{\gamma_1 - \gamma_3}{2} R - \gamma_2 R^3 - 2\eta R \cos(2\phi - \theta), \quad (\text{A8})$$

$$\dot{\phi} = \Delta + 2\eta \sin(2\phi - \theta). \quad (\text{A9})$$

When $\Delta < 2\eta$, the equation for the argument in Eq. (A9) has two stable fixed points $\phi_{ss} = \frac{1}{2} \left(\pi + \theta + \arcsin \left(\frac{\Delta}{2\eta} \right) \right)$ and $\phi_{ss} + \pi$. Additionally, when $\gamma_1 \geq \gamma_3$, or $\gamma_1 < \gamma_3$ and $\eta > \frac{1}{2} \sqrt{\frac{(\gamma_1 - \gamma_3)^2}{4} + \Delta^2}$, the equation for the modulus R has a non-zero solution $R_{ss} = \sqrt{\frac{1}{\gamma_2} \left(\frac{\gamma_1 - \gamma_3}{2} + \sqrt{4\eta^2 - \Delta^2} \right)}$, and consequently, the system in Eq. (A7) possesses two stable fixed points $\alpha_{ss} = \pm R_{ss} e^{i\phi_{ss}}$.

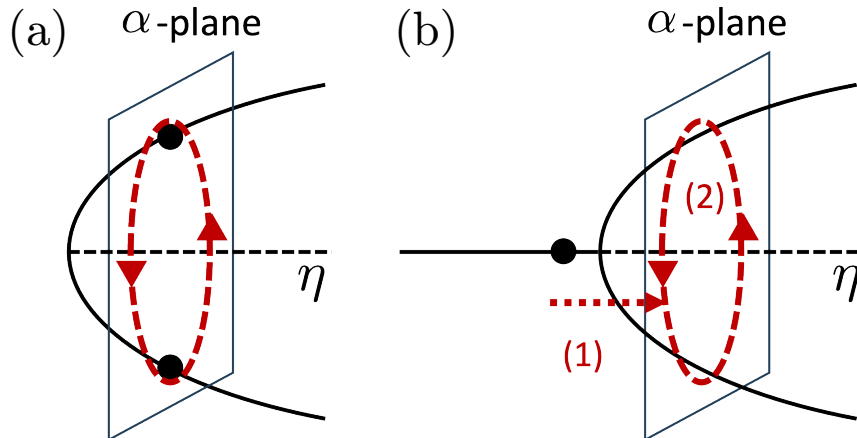


FIG. 6. A schematic diagram of noise-induced oscillations near the (a) SNIC bifurcation and (b) pitchfork bifurcation in the classical limit. In (b), the system exceeds the bifurcation points of the (1) modulus and (2) argument simultaneously.

Figs. 6 (a) and 6(b) schematically depict the bifurcation diagram when varying η for cases in Sec. III B and Sec. III C, respectively. In Sec. III B, the equation for the argument in Eq.(A9) is slightly below the bifurcation, i.e., $\Delta < 2\eta$, and the equation for the modulus

in Eq.(A8) always has two stable fixed points as $\gamma_1 > \gamma_3 (= 0)$. Then, as illustrated in Fig. 6(a), the oscillatory response is excited by the quantum noise, characterized by a round trip around the two stable fixed points. In Sec. III C, the equation for the argument in Eq.(A9) is slightly below the bifurcation, i.e., $\Delta < 2\eta$, and with $\gamma_3 > \gamma_1 (= 0)$, the equation for the modulus in Eq.(A8) is slightly below the bifurcation, i.e., $\eta < \frac{1}{2}\sqrt{\frac{(\gamma_1 - \gamma_3)^2}{4} + \Delta^2}$. Then, as illustrated in Fig. 6 (b), due to the quantum noise, the system exceeds the pitchfork bifurcation point of the modulus and two stable fixed points emerge, and simultaneously, the system exceeds the bifurcation point of the argument. As a result, the system exhibits oscillatory response of round trip around the two emerging stable fixed points. Thus, the system exhibits quantum noise-induced oscillations starting from the origin, arising because the system simultaneously exceeds the bifurcation points of both the modulus and argument.

Appendix B: Amplitude function of a harmonic oscillator with linear damping

In Ref.⁵¹, the stochastic asymptotic amplitude function for a classical stochastic damped harmonic oscillator was studied. In this appendix, building upon their findings, we calculate the quantum asymptotic amplitude for a simple quantum harmonic oscillator with linear damping. Although the system behaves linearly in the classical limit and does not exhibit nonlinear oscillations, we can still introduce the asymptotic amplitude function, as defined in Sec. II D.

In this setting, we can analytically obtain the eigenoperator V_2 of the adjoint Liouville operator \mathcal{L}^* . The quantum master equation of a damped harmonic oscillator is given by

$$\dot{\rho} = \mathcal{L}\rho = -i[\omega_0 a^\dagger a, \rho] + \gamma_3 \mathcal{D}[a]\rho. \quad (\text{B1})$$

For simplicity, we assume $\omega_0 \neq 0$ and the system is oscillatory.

The eigenoperator associated with the largest non-zero eigenvalue on the real axis of the adjoint Liouville operator \mathcal{L}^* is explicitly obtained as $V_2 = a^\dagger a$, i.e., $\mathcal{L}^* a^\dagger a = \kappa_q a^\dagger a$ with $\kappa_q = -\gamma_3$ ^{73,74}. Therefore, the quantum asymptotic amplitude function $R_q(\boldsymbol{\alpha})$ of the coherent state $\boldsymbol{\alpha}$ is given by

$$R_q(\boldsymbol{\alpha}) = \langle \alpha | a^\dagger a | \alpha \rangle = |\alpha|^2, \quad (\text{B2})$$

and the asymptotic amplitude function $R_q(\rho)$ of the density operator ρ is given by

$$R_q(\rho) = \langle a^\dagger a \rangle_q = \langle \rho, a^\dagger a \rangle_{tr} \left(= \int |\alpha|^2 p(\alpha) d\alpha \right). \quad (\text{B3})$$

For the initial condition $\rho_0 = |\alpha_0\rangle\langle\alpha_0|$ with $\alpha_0 = r_0 e^{i\theta_0}$, the expectation of $a^\dagger a$ evolves as

$$\frac{d}{dt} \langle a^\dagger a \rangle_q = \langle \dot{\rho}, a^\dagger a \rangle_{tr} = \langle \mathcal{L}\rho, a^\dagger a \rangle_{tr} = \langle \rho, \mathcal{L}^* a^\dagger a \rangle_{tr} = \kappa_q \langle \rho, a^\dagger a \rangle_{tr} = \kappa_q \langle a^\dagger a \rangle_q, \quad (\text{B4})$$

which yields $\langle a^\dagger a \rangle_q = e^{\kappa_q t} \langle \rho_0, a^\dagger a \rangle_{tr} = e^{\kappa_q t} \langle \alpha_0 | a^\dagger a | \alpha_0 \rangle = e^{\kappa_q t} |\alpha_0|^2 = e^{-\gamma_3 t} r_0^2$.

Thus, the asymptotic amplitude of the state ρ is obtained as

$$R_q(\rho) = e^{-\gamma_3 t} r_0^2, \quad (\text{B5})$$

which decays exponentially to zero with a constant rate γ_3 . Consequently, the zero level-set of the asymptotic amplitude forms a stable fixed point at the origin, and the effective quantum periodic orbit χ_q is absent in this case.

As in the example of a quantum harmonic oscillator with linear damping, the asymptotic amplitude function can be formally introduced for a wide variety of systems, even if the system lacks nonlinear oscillatory dynamics.

REFERENCES

- ¹Arthur T Winfree. The geometry of biological time. Springer, New York, 2001.
- ²Yoshiki Kuramoto. Chemical oscillations, waves, and turbulence. Springer, Berlin, 1984.
- ³Arkady Pikovsky, Michael Rosenblum, and Jürgen Kurths. Synchronization: a universal concept in nonlinear sciences. Cambridge University Press, Cambridge, 2001.
- ⁴Hiroya Nakao. Phase reduction approach to synchronisation of nonlinear oscillators. Contemporary Physics, 57(2):188–214, 2016.
- ⁵G Bard Ermentrout and David H Terman. Mathematical foundations of neuroscience. Springer, New York, 2010.
- ⁶SH Strogatz. Nonlinear dynamics and chaos. Westview Press, 1994.
- ⁷Tony E Lee and HR Sadeghpour. Quantum synchronization of quantum van der Pol oscillators with trapped ions. Physical Review Letters, 111(23):234101, 2013.
- ⁸Stefan Walter, Andreas Nunnenkamp, and Christoph Bruder. Quantum synchronization of a driven self-sustained oscillator. Physical Review Letters, 112(9):094102, 2014.

- ⁹Sameer Sonar, Michal Hajdušek, Manas Mukherjee, Rosario Fazio, Vlatko Vedral, Sai Vinjanampathy, and Leong-Chuan Kwek. Squeezing enhances quantum synchronization. Physical Review Letters, 120(16):163601, 2018.
- ¹⁰Tony E Lee, Ching-Kit Chan, and Shenshen Wang. Entanglement tongue and quantum synchronization of disordered oscillators. Physical Review E, 89(2):022913, 2014.
- ¹¹Yuzuru Kato, Naoki Yamamoto, and Hiroya Nakao. Semiclassical phase reduction theory for quantum synchronization. Physical Review Research, 1(3):033012, 2019.
- ¹²Niels Lörch, Ehud Amitai, Andreas Nunnenkamp, and Christoph Bruder. Genuine quantum signatures in synchronization of anharmonic self-oscillators. Physical Review Letters, 117(7):073601, 2016.
- ¹³W-K Mok, L-C Kwek, and H Heimonen. Synchronization boost with single-photon dissipation in the deep quantum regime. Physical Review Research, 2(3):033422, 2020.
- ¹⁴Dirk Witthaut, Sandro Wimberger, Raffaella Burioni, and Marc Timme. Classical synchronization indicates persistent entanglement in isolated quantum systems. Nature Communications, 8:14829, 2017.
- ¹⁵Alexandre Roulet and Christoph Bruder. Quantum synchronization and entanglement generation. Physical Review Letters, 121(6):063601, 2018.
- ¹⁶Niels Lörch, Simon E Nigg, Andreas Nunnenkamp, Rakesh P Tiwari, and Christoph Bruder. Quantum synchronization blockade: Energy quantization hinders synchronization of identical oscillators. Physical Review Letters, 118(24):243602, 2017.
- ¹⁷Talitha Weiss, Andreas Kronwald, and Florian Marquardt. Noise-induced transitions in optomechanical synchronization. New Journal of Physics, 18(1):013043, 2016.
- ¹⁸Najmeh Es' haqi Sani, Gonzalo Manzano, Roberta Zambrini, and Rosario Fazio. Synchronization along quantum trajectories. Physical Review Research, 2(2):023101, 2020.
- ¹⁹Yuzuru Kato and Hiroya Nakao. Enhancement of quantum synchronization via continuous measurement and feedback control. New Journal of Physics, 23(1):013007, 2021.
- ²⁰Wenlin Li, Najmeh Es' haqi Sani, Wen-Zhao Zhang, and David Vitali. Quantum zeno effect in self-sustaining systems: Suppressing phase diffusion via repeated measurements. Physical Review A, 103(4):043715, 2021.
- ²¹Yuzuru Kato and Hiroya Nakao. Semiclassical optimization of entrainment stability and phase coherence in weakly forced quantum limit-cycle oscillators. Physical Review E, 101(1):012210, 2020.

- ²²Michael R Hush, Weibin Li, Sam Genway, Igor Lesanovsky, and Andrew D Armour. Spin correlations as a probe of quantum synchronization in trapped-ion phonon lasers. Physical Review A, 91(6):061401, 2015.
- ²³Talitha Weiss, Stefan Walter, and Florian Marquardt. Quantum-coherent phase oscillations in synchronization. Physical Review A, 95(4):041802, 2017.
- ²⁴A Mari, A Farace, N Didier, V Giovannetti, and R Fazio. Measures of quantum synchronization in continuous variable systems. Physical Review Letters, 111(10):103605, 2013.
- ²⁵Minghui Xu, David A Tieri, EC Fine, James K Thompson, and Murray J Holland. Synchronization of two ensembles of atoms. Physical Review Letters, 113(15):154101, 2014.
- ²⁶Alexandre Roulet and Christoph Bruder. Synchronizing the smallest possible system. Physical Review Letters, 121(6):053601, 2018.
- ²⁷A Chia, LC Kwek, and C Noh. Relaxation oscillations and frequency entrainment in quantum mechanics. Physical Review E, 102(4):042213, 2020.
- ²⁸Lior Ben Arosh, MC Cross, and Ron Lifshitz. Quantum limit cycles and the rayleigh and van der Pol oscillators. Physical Review Research, 3(1):013130, 2021.
- ²⁹Noufal Jaseem, Michal Hajdušek, Parvinder Solanki, Leong-Chuan Kwek, Rosario Fazio, and Sai Vinjanampathy. Generalized measure of quantum synchronization. Physical Review Research, 2(4):043287, 2020.
- ³⁰Noufal Jaseem, Michal Hajdušek, Vlatko Vedral, Rosario Fazio, Leong-Chuan Kwek, and Sai Vinjanampathy. Quantum synchronization in nanoscale heat engines. Physical Review E, 101(2):020201, 2020.
- ³¹Albert Cabot, Gian Luca Giorgi, and Roberta Zambrini. Metastable quantum entrainment. New Journal of Physics, 23(10):103017, 2021.
- ³²Yuzuru Kato and Hiroya Nakao. A definition of the asymptotic phase for quantum nonlinear oscillators from the Koopman operator viewpoint. Chaos: An Interdisciplinary Journal of Nonlinear Science, 32(6):063133, 2022.
- ³³Yuzuru Kato and Hiroya Nakao. Quantum asymptotic phases reveal signatures of quantum synchronization. New Journal of Physics, 25(2):023012, 2023.
- ³⁴Wataru Setoyama and Yoshihiko Hasegawa. Lie algebraic quantum phase reduction. Physical Review Letters, 132(9):093602, 2024.
- ³⁵Biswabibek Bandyopadhyay and Tanmoy Banerjee. Aging transition in coupled quantum oscillators. Physical Review E, 107(2):024204, 2023.

- ³⁶Arif Warsi Laskar, Pratik Adhikary, Suprodip Mondal, Parag Katiyar, Sai Vinjanampathy, and Saikat Ghosh. Observation of quantum phase synchronization in spin-1 atoms. Physical Review Letters, 125(1):013601, 2020.
- ³⁷VR Krithika, Parvinder Solanki, Sai Vinjanampathy, and TS Mahesh. Observation of quantum phase synchronization in a nuclear-spin system. Physical Review A, 105(6):062206, 2022.
- ³⁸Martin Koppenhöfer, Christoph Bruder, and Alexandre Roulet. Quantum synchronization on the IBM Q system. Physical Review Research, 2(2):023026, 2020.
- ³⁹Arthur T Winfree. Biological rhythms and the behavior of populations of coupled oscillators. Journal of Theoretical Biology, 16(1):15–42, 1967.
- ⁴⁰John Guckenheimer. Isochrons and phaseless sets. Journal of Mathematical Biology, 1:259–273, 1975.
- ⁴¹Alexandre Mauroy, Igor Mezić, and Jeff Moehlis. Isostables, isochrons, and Koopman spectrum for the action–angle representation of stable fixed point dynamics. Physica D: Nonlinear Phenomena, 261:19–30, 2013.
- ⁴²Sho Shirasaka, Wataru Kurebayashi, and Hiroya Nakao. Phase-amplitude reduction of transient dynamics far from attractors for limit-cycling systems. Chaos, 27(2):023119, 2017.
- ⁴³Alexandre Mauroy, Y Susuki, and I Mezić. Koopman operator in systems and control. Springer, 2020.
- ⁴⁴Yoshiki Kuramoto and Hiroya Nakao. On the concept of dynamical reduction: the case of coupled oscillators. Philosophical Transactions of the Royal Society A, 377(2160):20190041, 2019.
- ⁴⁵Alexandre Mauroy and Igor Mezić. Global computation of phase-amplitude reduction for limit-cycle dynamics. Chaos: An Interdisciplinary Journal of Nonlinear Science, 28(7):073108, 2018.
- ⁴⁶Sho Shirasaka, Wataru Kurebayashi, and Hiroya Nakao. Phase-amplitude reduction of limit cycling systems. In The Koopman Operator in Systems and Control, pages 383–417. Springer, 2020.
- ⁴⁷Matthew D Kvalheim and Shai Revzen. Existence and uniqueness of global koopman eigenfunctions for stable fixed points and periodic orbits. Physica D: Nonlinear Phenomena, 425:132959, 2021.

- ⁴⁸Bharat Monga, Dan Wilson, Tim Matchen, and Jeff Moehlis. Phase reduction and phase-based optimal control for biological systems: a tutorial. Biological Cybernetics, 113(1-2):11–46, 2019.
- ⁴⁹Dan Wilson and Jeff Moehlis. Isostable reduction of periodic orbits. Physical Review E, 94(5):052213, 2016.
- ⁵⁰Peter J Thomas and Benjamin Lindner. Asymptotic phase for stochastic oscillators. Physical Review Letters, 113(25):254101, 2014.
- ⁵¹Alberto Pérez-Cervera, Benjamin Lindner, and Peter J Thomas. Isostables for stochastic oscillators. Physical Review Letters, 127(25):254101, 2021.
- ⁵²Oliver Junge, Jerrold E Marsden, and Igor Mezic. Uncertainty in the dynamics of conservative maps. In 2004 43rd IEEE Conference on Decision and Control (CDC)(IEEE Cat. No. 04CH37601), volume 2, pages 2225–2230. IEEE, 2004.
- ⁵³Nelida Črnjarić-Žic, Senka Maćešić, and Igor Mezić. Koopman operator spectrum for random dynamical systems. Journal of Nonlinear Science, 30(5):2007–2056, 2020.
- ⁵⁴Mathias Thomas Wanner. Robust Approximation of the Stochastic Koopman Operator. University of California, Santa Barbara, 2020.
- ⁵⁵Yuzuru Kato, Jinjie Zhu, Wataru Kurebayashi, and Hiroya Nakao. Asymptotic phase and amplitude for classical and semiclassical stochastic oscillators via Koopman operator theory. Mathematics, 9(18):2188, 2021.
- ⁵⁶Howard J Carmichael. Statistical Methods in Quantum Optics 1, 2. Springer, New York, 2007.
- ⁵⁷Crispin W Gardiner. Quantum Noise. Springer, New York, 1991.
- ⁵⁸Heinz-Peter Breuer, Francesco Petruccione, et al. The theory of open quantum systems. Oxford University Press on Demand, 2002.
- ⁵⁹Daniel A Lidar, Isaac L Chuang, and K Birgitta Whaley. Decoherence-free subspaces for quantum computation. Physical Review Letters, 81(12):2594, 1998.
- ⁶⁰Kevin E Cahill and Roy J Glauber. Density operators and quasiprobability distributions. Physical Review, 177(5):1882, 1969.
- ⁶¹John Guckenheimer and Philip Holmes. Nonlinear Oscillations, Dynamical Systems, and Bifurcations of Vector Fields. Springer, 1983.
- ⁶²Yuzuru Kato and Hiroya Nakao. Quantum coherence resonance. New Journal of Physics, 2021.

- ⁶³Nikolas Tezak, Nina H Amini, and Hideo Mabuchi. Low-dimensional manifolds for exact representation of open quantum systems. Physical Review A, 96(6):062113, 2017.
- ⁶⁴Yuzuru Kato and Hiroya Nakao. Turing instability in quantum activator–inhibitor systems. Scientific Reports, 12(1):15573, 2022.
- ⁶⁵Heather A Brooks and Paul C Bressloff. Quasicycles in the stochastic hybrid morris-lecar neural model. Physical Review E, 92(1):012704, 2015.
- ⁶⁶Mark C Cross and Pierre C Hohenberg. Pattern formation outside of equilibrium. Reviews of modern physics, 65(3):851, 1993.
- ⁶⁷Alberto Pérez-Cervera, Boris Gutkin, Peter J Thomas, and Benjamin Lindner. A universal description of stochastic oscillators. Proceedings of the National Academy of Sciences, 120(29):e2303222120, 2023.
- ⁶⁸Shovan Dutta, Shu Zhang, and Masudul Haque. Quantum origin of limit cycles, fixed points, and critical slowing down. Physical Review Letters, 134(5):050407, 2025.
- ⁶⁹Yuzuru Kato and Hiroya Nakao. Quantum spin van der pol oscillator—a spin-based limit-cycle oscillator exhibiting quantum synchronization. arXiv preprint arXiv:2409.08791, 2024.
- ⁷⁰Bernard O Koopman. Hamiltonian systems and transformation in hilbert space. Proceedings of the National Academy of Sciences, 17(5):315–318, 1931.
- ⁷¹JR Johansson, PD Nation, and Franco Nori. Qutip: An open-source python framework for the dynamics of open quantum systems. Computer Physics Communications, 183(8):1760–1772, 2012.
- ⁷²JR Johansson, PD Nation, and Franco Nori. Qutip 2: A python framework for the dynamics of open quantum systems. Computer Physics Communications, 184:1234–1240, 2013.
- ⁷³Stephen M Barnett and Stig Stenholm. Spectral decomposition of the lindblad operator. Journal of Modern Optics, 47(14-15):2869–2882, 2000.
- ⁷⁴Hans-Jürgen Briegel and Berthold-Georg Englert. Quantum optical master equations: The use of damping bases. Physical Review A, 47(4):3311, 1993.